

# Cross-Domain Structure Preserving Projection for Heterogeneous Domain Adaptation

Qian Wang, Toby P. Breckon

Department of Computer Science, Durham University, UK.  
*qian.wang173@hotmail.com, toby.breckon@durham.ac.uk*

## Abstract

Heterogeneous Domain Adaptation (HDA) addresses the transfer learning problems where data from the source and target domains are of different modalities (e.g., texts and images) or feature dimensions (e.g., features extracted with different methods). It is useful for multi-modal data analysis. Traditional domain adaptation algorithms assume that the representations of source and target samples reside in the same feature space, hence are likely to fail in solving the heterogeneous domain adaptation problem. Contemporary state-of-the-art HDA approaches are usually composed of complex optimization objectives for favourable performance and are therefore computationally expensive and less generalizable. To address these issues, we propose a novel Cross-Domain Structure Preserving Projection (CDSPP) algorithm for HDA. As an extension of the classic LPP to heterogeneous domains, CDSPP aims to learn domain-specific projections to map sample features from source and target domains into a common subspace such that the class consistency is preserved and data distributions are sufficiently aligned. CDSPP is simple and has deterministic solutions by solving a generalized eigenvalue problem. It is naturally suitable for supervised HDA but has also been extended for semi-supervised HDA where the unlabeled target domain samples are available. Extensive experiments have been conducted on commonly used benchmark datasets (i.e. Office-Caltech, Multilingual Reuters Collection, NUS-WIDE-ImageNet) for HDA as well as the Office-Home dataset firstly introduced for HDA by ourselves due to its significantly larger number of classes than the existing ones (65 vs 10, 6 and 8). The experimental results of both supervised and semi-supervised HDA demonstrate the superior performance of our proposed method against contemporary state-of-the-art methods.

**Keywords:** heterogeneous domain adaptation, cross-domain projection, image classification, text classification

## 1. Introduction

Supervised learning can achieve good performance given considerable amounts of labeled data for training. One essential factor accounting for the recent successes in deep learning and image classification is the ImageNet database which contains more than 14 million hand-annotated images [7]. However, there exist many tasks in real-world applications where sufficient labeled data are not available, hence the performance of traditional supervised learning approaches can degrade significantly. One promising technique alleviating this problem is transfer learning which aims to transfer knowledge learned from the source domain to the target domain in which labeled data are sparse and expensive to collect [31]. In many scenarios, domain adaptation is required since the data distributions in the source and target domains can be different and the models trained with source domain data are not directly applicable to the target domain [21].

Since domain adaptation is a promising solution to the training data sparsity issue in many real-world applications, it has been studied in a variety of research tasks including image classification [29], semantic segmentation [35], depth estimation [2], speech emotion recognition [36], text classification [38] and many others.

Domain adaptation approaches aim to model the domain shift between source and target domains and reduce the discrepancy

by aligning the data distributions [29, 28]. In the scope of classification problems, this is usually boiled down to aligning the marginal and class conditional distributions across domains [27, 3]. However, most existing works are based on the assumption of homogeneity, i.e., the source and target data are represented in the same feature space with unaligned distributions [35, 29, 34, 28]. These approaches may not be applicable in the situations where source and target domains are *heterogeneous* in the forms of data modalities (e.g., texts vs images) or representations (e.g., features extracted with different methods).

In this work, we address the heterogeneous domain adaptation problem where source and target data are represented in heterogeneous feature spaces. Following the same spirits of previous domain adaptation approaches [27, 29, 28], we try to learn a common latent subspace where both source and target data can be projected and well aligned in the learnt subspace. Specifically, we learn domain-specific projections using a novel Cross-Domain Structure Preserving Projection (CDSPP) algorithm which is an extension of the classic Locality Preserving Projection (LPP) algorithm [12]. CDSPP is able to facilitate the class consistency preserving to learn domain-specific projections which can be used to map heterogeneous data representations into a common subspace for recognition. CDSPP is simple yet effective in solving the heterogeneous domain adaptation problem as empirically validated by our experimental results on several benchmark datasets. The contributions of this

work can be summarised as follows:

- A novel Cross-Domain Structure Preserving Projection algorithm is proposed for heterogeneous domain adaptation and the algorithm has a concise solution by solving a generalized eigenvalue problem;
- The proposed CDSPP algorithm is naturally for supervised HDA and we extend it to solve the semi-supervised HDA problems by employing an iterative pseudo-labeling approach;
- We validate the effectiveness of the proposed method on several benchmark datasets including the newly introduced Office-Home which contains much more classes than the previously used ones; the experimental results provide evidence our algorithm outperforms prior art.

## 2. Related Work

Most exiting research in domain adaptation for classification is based on the assumption of homogeneity. The approaches are dedicated to either learning a domain-invariant feature extraction model (e.g., deep CNN [4, 34]) or learning a unified feature projection matrix [27, 29, 28] for all domains whilst neither of them is applicable to HDA. In this section, we briefly review related works on heterogeneous domain adaptation. The existing approaches to HDA can be roughly categorized into *cross-domain mapping* and *common subspace learning*.

### 2.1. Cross-Domain Mapping

Cross-domain mapping approaches learn a projection from the source to the target domain. The projection can be learned for either *feature transformation* [14, 23] or *model parameter transformation* (e.g., SVM weights [38, 20]). Feature transformation approaches learn a projection to map the source data into the target data by aligning the data distribution [14] or the second-order moment [23]. As a result, the transformed source data can help to learn a classifier for the target domain. To avoid mapping a lower-dimensional feature to a higher-dimensional space, PCA is usually employed to learn subspaces for both domains respectively [14] as a pre-processing which can suffer from information loss.

Model parameter transformation approaches focus mainly on SVM classifier weights. For a multi-class classification problem, one-vs-all classifiers are learned for source and target domains using the respective labeled samples. Subsequently, the cross-domain mapping is learned from the paired class-level weight vectors [38, 20]. Since the number of classes is far less than the number of samples, these approaches are more computationally efficient but rely too much on the learned classifiers and overlooked abundant information underlying the data distribution.

### 2.2. Common Subspace Learning

Common subspace learning is a more popular strategy for HDA. It learns domain-specific projections which map source and target domain data into a common subspace. To this end, different approaches have been proposed with varying algorithms, e.g., Manifold Alignment [26, 17, 9], Canonical Correlation Analysis [32], Coding Space Learning [18, 16, 8], Deep Matrix Completion [15] and Deep Neural Networks [37, 33]. In spite of the diversity of implementation, the main objective of common subspace learning based HDA is similar, i.e., the alignment of the source and target domains.

To align the distributions, [14, 18, 16, 17, 15] chose to minimize the Maximum Mean Discrepancy (MMD) in their objectives which, however, can only align the means of domains (for marginal distributions) and the means of classes (for conditional distributions). As a result, the subspace learned via minimizing the MMD is not sufficiently discriminative. One alternative to MMD is the manifold learning using graph Laplacian [26, 16, 17].

Li et al. [19] proposed a Heterogeneous Feature Augmentation (HFA) method and its semi-supervised version SHFA by learning domain-specific projections and a classifier (i.e. SVM) simultaneously. However, the computational complexity is  $\mathcal{O}(n^3)$ , where  $n$  is the number of labeled samples and makes it extremely slow when  $n$  is large. Li et al. [18] learned new feature representations for source and target data by encoding them with a shared codebook which requires the original features have the same dimensions for source and target domains. PCA was employed for this purpose as a pre-processing but can suffer from information loss. Lately, the authors incorporated the learning of two domain-specific projections (in place of PCA) into the coding framework [16]. This work is similar to ours in the sense of local consistency using the graph regularization, however, it fails to align cross-domain class consistency due to the use of  $k$  nearest neighbours to construct the similarity graph. In our work, the similarity graph is constructed based on class consistency, hence promoting the cross-domain conditional distribution alignment.

Transfer Independently Together (TIT) was proposed in [17]. It also learns domain-specific projections to align data distributions in the learned common subspace. The algorithm was based on a collection of tricks including kernel space, MMD, sample reweighting and landmark selection. In contrast, our solution is concise with one simple objective of cross-domain structure preserving. Recently, Huang et al. [13] proposed a novel algorithm, named as heterogeneous discriminative features learning and label propagation (HDL). This algorithm is similar to ours in that both tend to preserve structure information in the learned common subspace. However, different objectives have been formulated. Our algorithm explicitly promotes the intra-class similarity for both within-domain and cross-domain samples, whilst HDL fails to consider the intra-class similarity for samples from the same domain in their formulation. In addition, different strategies of unlabeled target sample exploration were employed in two algorithms.

In summary, although manifold learning has been well studied in HDA, the existing formulations for domain-specific pro-

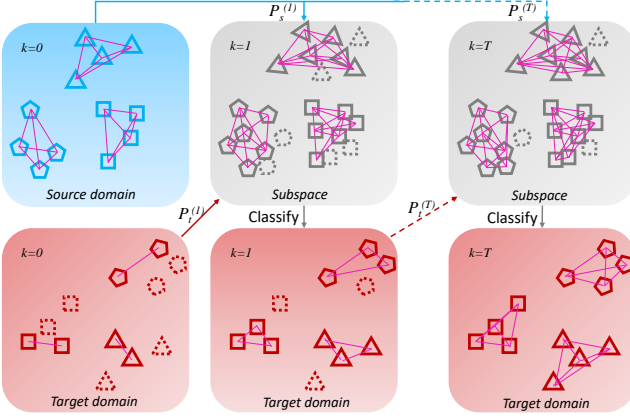


Figure 1: The framework of our proposed approach (the red and the blue colors are used to represent target and source domains respectively; markers of different shapes represent samples from different classes; dashed markers represent unlabeled samples).

jection learning are either inefficient or ineffective. Our approach solves this issue and addresses the HDA problem with a novel CDSPP algorithm.

### 3. Method

To facilitate our presentation, we firstly describe the heterogeneous domain adaptation problem and notations used throughout this paper. Given a labeled dataset  $\mathcal{D}^s = \{(\mathbf{x}_i^s, y_i^s)\}, i = 1, 2, \dots, n_s$  from the source domain  $\mathcal{S}$ , and a labeled dataset  $\mathcal{D}^t = \{(\mathbf{x}_i^t, y_i^t)\}, i = 1, 2, \dots, n_t$  from the target domain,  $\mathbf{x}_i^s \in \mathbb{R}^{d_s}$  and  $\mathbf{x}_i^t \in \mathbb{R}^{d_t}$  represent the feature vectors of  $i$ -th labeled samples in the source and target domains respectively;  $d_s$  and  $d_t$  are the dimensionalities of the source and target features;  $y_i^s \in \mathcal{Y}$  and  $y_i^t \in \mathcal{Y}$  denote the corresponding sample labels;  $n_s$  and  $n_t$  are the number of source and labeled target samples respectively. Let  $\mathbf{X}^s \in \mathbb{R}^{d_s \times n_s}$  and  $\mathbf{X}^t \in \mathbb{R}^{d_t \times n_t}$  be the feature matrices of labeled source and target data collectively, supervised HDA aims to learn a model from labeled source and target data, which can be used to classify samples from an unlabeled dataset  $\mathcal{D}^u = \{\mathbf{x}_i^u\}, i = 1, 2, \dots, n_u$  from the target domain, whose feature vectors can be collectively denoted as  $\mathbf{X}^u \in \mathbb{R}^{d_t \times n_u}$ .

The number of labeled target samples  $n_t$  is usually very small, hence it is difficult to capture the data distribution in the target domain. Semi-supervised HDA takes advantage of the unlabeled target samples  $\mathbf{X}^u$  during model training and can usually achieve better performance.

In this section, we describe the CDSPP algorithm which is naturally for supervised heterogeneous domain adaptation, but can be used to address the semi-supervised heterogeneous domain adaptation problem by incorporating it into an iterative learning framework [29, 28] as shown in Figure 1.

#### 3.1. Cross-Domain Structure Preserving Projection

Locality Preserving Projection (LPP) was proposed by He and Niyogi [12] to learn a favorable subspace where the local structures of data in the original feature space can be well

preserved. The supervised version of LPP [30] was proved to be able to learn a subspace of better separability than other dimensionality reduction algorithms such as Linear Discriminant Analysis (LDA) [29]. One limitation of LPP is that it can only learn the subspace from samples represented in a homogeneous feature space. To address this problem, we extend the traditional LPP so that its favourable characteristics can benefit cross-domain common subspace learning. Specifically, we aim to learn a projection matrix  $\mathbf{P}_s \in \mathbb{R}^{d_s \times d}$  for the source domain and a projection matrix  $\mathbf{P}_t \in \mathbb{R}^{d_t \times d}$  for the target domain to project the samples from source and target domains into a common subspace whose dimensionality is  $d$ . We expect the samples projections are close to one another if they are from the same class regardless which domain they are from. To this end, we have the following objective:

$$\begin{aligned} \min_{\mathbf{P}_s, \mathbf{P}_t} \quad & (\sum_{i,j}^{n_s} \|\mathbf{P}_s^T \mathbf{x}_i^s - \mathbf{P}_s^T \mathbf{x}_j^s\|_2^2 \mathbf{W}_{ij}^s \\ & + \sum_i^{n_s} \sum_j^{n_t} \|\mathbf{P}_s^T \mathbf{x}_i^s - \mathbf{P}_t^T \mathbf{x}_j^t\|_2^2 \mathbf{W}_{ij}^c \\ & + \sum_{i,j}^{n_t} \|\mathbf{P}_t^T \mathbf{x}_i^t - \mathbf{P}_t^T \mathbf{x}_j^t\|_2^2 \mathbf{W}_{ij}^t) \end{aligned} \quad (1)$$

where  $\mathbf{P}^T$  is the transpose of  $\mathbf{P}$ ;  $\mathbf{W}^s \in \mathbb{R}^{n_s \times n_s}$  is the similarity matrix of the source samples and  $\mathbf{W}_{ij}^s = 1$  if  $y_i^s = y_j^s$ , 0 otherwise. Similarly,  $\mathbf{W}^t \in \mathbb{R}^{n_t \times n_t}$  is the similarity matrix of the labeled target samples and  $\mathbf{W}_{ij}^t = 1$  if  $y_i^t = y_j^t$ , 0 otherwise.  $\mathbf{W}^c \in \mathbb{R}^{n_s \times n_t}$  is the cross-domain similarity matrix and  $\mathbf{W}_{ij}^c = 1$  if  $y_i^s = y_j^t$ , 0 otherwise.

**Proposition 3.1.** *The objective in Eq.(1) can be reformulated as follows:*

$$\max_{\mathbf{P}_s, \mathbf{P}_t} \frac{\text{tr}(\mathbf{X}^{sT} \mathbf{P}_s \mathbf{P}_t^T \mathbf{X}^t \mathbf{W}^{cT})}{\text{tr}(\mathbf{X}^{sT} \mathbf{P}_s \mathbf{P}_s^T \mathbf{X}^s \mathbf{L}^s) + \text{tr}(\mathbf{X}^{tT} \mathbf{P}_t \mathbf{P}_t^T \mathbf{X}^t \mathbf{L}^t)} \quad (2)$$

where  $\mathbf{L}^s = \mathbf{D}^s - \mathbf{W}^s + \frac{1}{2} \mathbf{D}^{cs}$  and  $\mathbf{L}^t = \mathbf{D}^t - \mathbf{W}^t + \frac{1}{2} \mathbf{D}^{ct}$ ;  $\mathbf{D}^s \in \mathbb{R}^{n_s \times n_s}$  is a diagonal matrix with  $\mathbf{D}_{ii}^s = \sum_j^{n_s} \mathbf{W}_{ij}^s$  and  $\mathbf{D}^t \in \mathbb{R}^{n_t \times n_t}$  is a diagonal matrix with  $\mathbf{D}_{jj}^t = \sum_i^{n_t} \mathbf{W}_{ij}^t$ ;  $\mathbf{D}^{cs} \in \mathbb{R}^{n_s \times n_s}$  is a diagonal matrix with  $\mathbf{D}_{ii}^{cs} = \sum_i^{n_t} \mathbf{W}_{ij}^c$  and  $\mathbf{D}^{ct} \in \mathbb{R}^{n_t \times n_t}$  is a diagonal matrix with  $\mathbf{D}_{jj}^{ct} = \sum_i^{n_s} \mathbf{W}_{ij}^c$ .

*Proof.* By firstly doing the binomial expansion then transforming it to the form of matrix multiplication and trace of matrices, the first term in Eq.(1) can be reformulated as follows:

$$\begin{aligned} & \sum_{i,j}^{n_s} \|\mathbf{P}_s^T \mathbf{x}_i^s - \mathbf{P}_s^T \mathbf{x}_j^s\|_2^2 \mathbf{W}_{ij}^s \\ & = \sum_{i,j}^{n_s} (\mathbf{x}_i^{sT} \mathbf{P}_s \mathbf{P}_s^T \mathbf{x}_i^s - 2\mathbf{x}_i^{sT} \mathbf{P}_s \mathbf{P}_s^T \mathbf{x}_j^s + \mathbf{x}_j^{sT} \mathbf{P}_s \mathbf{P}_s^T \mathbf{x}_j^s) \mathbf{W}_{ij}^s \\ & = 2 \sum_i^{n_s} \mathbf{x}_i^{sT} \mathbf{P}_s \mathbf{P}_s^T \mathbf{x}_i^s \mathbf{D}_{ii}^s - 2 \sum_{i,j}^{n_s} \mathbf{x}_i^{sT} \mathbf{P}_s \mathbf{P}_s^T \mathbf{x}_j^s \mathbf{W}_{ij}^s \\ & = 2 \text{tr}(\mathbf{X}^{sT} \mathbf{P}_s \mathbf{P}_s^T \mathbf{X}^s \mathbf{D}^s) - 2 \text{tr}(\mathbf{X}^{sT} \mathbf{P}_s \mathbf{P}_s^T \mathbf{X}^s \mathbf{W}^s) \end{aligned} \quad (3)$$

In the similar way, the third term in Eq.(1) can be rewritten as:

$$\begin{aligned} & \sum_{i,j}^{n_t} \|\mathbf{P}_t^T \mathbf{x}_i^t - \mathbf{P}_t^T \mathbf{x}_j^t\|_2^2 \mathbf{W}_{ij}^t \\ & = 2 \text{tr}(\mathbf{X}^{tT} \mathbf{P}_t \mathbf{P}_t^T \mathbf{X}^t \mathbf{D}^t) - 2 \text{tr}(\mathbf{X}^{tT} \mathbf{P}_t \mathbf{P}_t^T \mathbf{X}^t \mathbf{W}^t) \end{aligned} \quad (4)$$

The second term in Eq.(1) can be rewritten as:

$$\begin{aligned}
& \sum_i^{n_s} \sum_j^{n_t} \|\mathbf{P}_s^T \mathbf{x}_i^s - \mathbf{P}_t^T \mathbf{x}_j^t\|_2^2 \mathbf{W}_{ij}^c \\
&= \sum_i^{n_s} \sum_j^{n_t} (\mathbf{x}_i^s \mathbf{P}_s \mathbf{P}_s^T \mathbf{x}_i^s - 2\mathbf{x}_i^s \mathbf{P}_s \mathbf{P}_t^T \mathbf{x}_j^t \\
&\quad + \mathbf{x}_j^T \mathbf{P}_t \mathbf{P}_t^T \mathbf{x}_j^t) \mathbf{W}_{ij}^c \\
&= \sum_i^{n_s} \mathbf{x}_i^s \mathbf{P}_s \mathbf{P}_s^T \mathbf{x}_i^s \mathbf{D}_{ii}^{cs} - 2 \sum_i^{n_s} \sum_j^{n_t} \mathbf{x}_i^s \mathbf{P}_s \mathbf{P}_t^T \mathbf{x}_j^t \mathbf{W}_{ij}^c \\
&\quad + \sum_j^{n_t} \mathbf{x}_j^T \mathbf{P}_t \mathbf{P}_t^T \mathbf{x}_j^t \mathbf{D}_{jj}^{ct} \\
&= \text{tr}(\mathbf{X}^s \mathbf{P}_s \mathbf{P}_s^T \mathbf{X}^s \mathbf{D}^{cs}) - 2 \text{tr}(\mathbf{X}^s \mathbf{P}_s \mathbf{P}_t^T \mathbf{X}^t \mathbf{W}^{ct}) \\
&\quad + \text{tr}(\mathbf{X}^t \mathbf{P}_t \mathbf{P}_t^T \mathbf{X}^t \mathbf{D}^{ct})
\end{aligned} \tag{5}$$

Substitute Eqs.(3-5) into the objective Eq.(1), we have the following form of objective:

$$\begin{aligned}
& \min_{\mathbf{P}_s, \mathbf{P}_t} (\text{tr}(\mathbf{X}^s \mathbf{P}_s \mathbf{P}_s^T \mathbf{X}^s \mathbf{L}^s) + \text{tr}(\mathbf{X}^t \mathbf{P}_t \mathbf{P}_t^T \mathbf{X}^t \mathbf{L}^t) \\
& - \text{tr}(\mathbf{X}^s \mathbf{P}_s \mathbf{P}_t^T \mathbf{X}^t \mathbf{W}^{ct})) \tag{6}
\end{aligned}$$

where  $\mathbf{L}^s = \mathbf{D}^s - \mathbf{W}^s + \frac{1}{2} \mathbf{D}^{cs}$  and  $\mathbf{L}^t = \mathbf{D}^t - \mathbf{W}^t + \frac{1}{2} \mathbf{D}^{ct}$ .

Minimizing the objective in Eq.(6) is equivalent to maximizing the objective in Eq.(2).  $\square$

**Proposition 3.2.** *The objective in Eq.(2) is equivalent to the following generalized eigenvalue problem and the optimal projection matrix  $\mathbf{P} = \begin{bmatrix} \mathbf{P}_s \\ \mathbf{P}_t \end{bmatrix}$  can be formed by  $d$  eigenvectors corresponding to the largest  $d$  eigenvalues:*

$$\mathbf{A}\mathbf{P} = (\mathbf{B} + \alpha \mathbf{I})\mathbf{P}\Lambda \tag{7}$$

where  $\mathbf{I} \in \mathbb{R}^{(n_s+n_t) \times (n_s+n_t)}$  is an identity matrix,  $\alpha$  is a hyper-parameter for regularization [30],  $\Lambda$  is a diagonal eigenvalue matrix and

$$\mathbf{A} = \begin{bmatrix} \mathbf{0} & \mathbf{X}^s \mathbf{W}^c \mathbf{X}^t \\ \mathbf{X}^t \mathbf{W}^c \mathbf{X}^s & \mathbf{0} \end{bmatrix}, \tag{8}$$

$$\mathbf{B} = \begin{bmatrix} \mathbf{X}^s \mathbf{L}^s \mathbf{X}^s & \mathbf{0} \\ \mathbf{0} & \mathbf{X}^t \mathbf{L}^t \mathbf{X}^t \end{bmatrix}. \tag{9}$$

*Proof.* To make the proof process concise, we introduce notations  $\mathbf{S}_s = \mathbf{X}^s \mathbf{L}^s \mathbf{X}^s$ ,  $\mathbf{S}_t = \mathbf{X}^t \mathbf{L}^t \mathbf{X}^t$  and  $\mathbf{S}_c = \mathbf{X}^s \mathbf{W}^c \mathbf{X}^t$ .

Let

$$\mathcal{J}(\mathbf{P}_s, \mathbf{P}_t) = \frac{\text{tr}(\mathbf{P}_t^T \mathbf{S}_c \mathbf{P}_s)}{\text{tr}(\mathbf{P}_s^T \mathbf{S}_s \mathbf{P}_s) + \text{tr}(\mathbf{P}_t^T \mathbf{S}_t \mathbf{P}_t)} \tag{10}$$

be the objective function in Eq.(2), we calculate the partial derivatives [22] of  $\mathcal{J}$  w.r.t.  $\mathbf{P}_s$  and  $\mathbf{P}_t$  respectively, set them to 0 and get the following equations:

$$\mathbf{S}_c \mathbf{P}_t = \frac{2\text{tr}(\mathbf{P}_t^T \mathbf{S}_c \mathbf{P}_s)}{\text{tr}(\mathbf{P}_s^T \mathbf{S}_s \mathbf{P}_s) + \text{tr}(\mathbf{P}_t^T \mathbf{S}_t \mathbf{P}_t)} \mathbf{S}_s \mathbf{P}_s \tag{11}$$

$$\mathbf{S}_c^T \mathbf{P}_s = \frac{2\text{tr}(\mathbf{P}_t^T \mathbf{S}_c \mathbf{P}_s)}{\text{tr}(\mathbf{P}_s^T \mathbf{S}_s \mathbf{P}_s) + \text{tr}(\mathbf{P}_t^T \mathbf{S}_t \mathbf{P}_t)} \mathbf{S}_t \mathbf{P}_t \tag{12}$$

Note that the coefficients on the right side of Eqs.(11-12) are exactly the objective in Eq.(10). It is easy to construct the following generalized eigenvalue problem by combining Eqs.(11-12):

$$\begin{bmatrix} \mathbf{0} & \mathbf{S}_c \\ \mathbf{S}_c^T & \mathbf{0} \end{bmatrix} \begin{bmatrix} \mathbf{P}_s \\ \mathbf{P}_t \end{bmatrix} = \begin{bmatrix} \mathbf{S}_s & \mathbf{0} \\ \mathbf{0} & \mathbf{S}_t \end{bmatrix} \begin{bmatrix} \mathbf{P}_s \\ \mathbf{P}_t \end{bmatrix} \Lambda. \tag{13}$$

The maximum objective is given by the largest eigenvalue solution to the generalized eigenvalue problem [12] and the eigenvectors corresponding to the largest  $d$  eigenvalues will form the projection matrix  $\mathbf{P}_s$  and  $\mathbf{P}_t$ .  $\square$

### 3.2. Recognition in the Subspace

Once the projection matrices  $\mathbf{P}_s$  and  $\mathbf{P}_t$  are learned, we are able to project all the labeled samples into the learned common subspace by  $\mathbf{z}_i^s = \mathbf{P}_s^T \mathbf{x}_i^s$  and  $\mathbf{z}_i^t = \mathbf{P}_t^T \mathbf{x}_i^t$ . For each class, we calculate the class mean  $\bar{\mathbf{z}}_c$  for  $c = 1, 2, \dots, C$  using all the labeled sample from both source and target domains. Given an unlabeled target sample  $\mathbf{x}^u$ , we classify it to the closest class in terms of its Euclidean distances to the class means:

$$y^* = \arg \min_c d(\bar{\mathbf{z}}_c, \mathbf{P}_t^T \mathbf{x}^u) \tag{14}$$

**Relation to DAMA** The CDSPP algorithm is quite similar to DAMA proposed in [26] at the first glance, however, they are essentially different from each other in that CDSPP does not seek to push the sample projections belonging to different classes apart, since the penalty imposed for this purpose (e.g., maximizing the term  $B$  in [26]) might misguide the solution to focus too much on the separation of classes which are originally close to each other and hurt the overall separability of the learned subspace. In contrast, our objective in Eq.(1) can guarantee the separability of the learned subspace by promoting the preserving of cluster structures underlying the original data distributions, which is simpler but more effective as validated by experiments.

### 3.3. Extending to Semi-Supervised HDA

The CDSPP algorithm is naturally suitable for supervised HDA but can be extended to semi-supervised HDA by incorporating it into an iterative pseudo-labeling framework [29]. Given a set of unlabeled target samples  $\mathbf{X}^u$ , they can be labeled by Eq.(14). The pseudo-labeled target samples can be used to update the projection matrices  $\mathbf{P}_s$  and  $\mathbf{P}_t$ . However, when the domain shift is large and the number of labeled target samples is limited, the pseudo-labels can be wrong for a considerable number of target samples. In this case, the mistakenly pseudo-labeled target samples might have a negative effect on projection learning. To reduce this risk, confidence aware pseudo-labeling is proposed in [29]. We employ the same idea and progressively select the most confidently pseudo-labeled target samples for the next iteration of CDSPP learning. The algorithms of supervised and semi-supervised HDA are summarized in Algorithm 1

### 3.4. Complexity Analysis

The time complexity of CDSPP is mainly contributed by two parts: the matrix multiplications in Eqs.(8-9) and the eigen decomposition problem. The complexity of matrix multiplications is  $\mathcal{O}((n_s + n_t)d_s d_t)$ . The complexity of eigen decomposition is generally  $\mathcal{O}((d_s + d_t)^3)$ . As a result, the CDSPP algorithm has a complexity of  $\mathcal{O}((n_s + n_t)d_s d_t + (d_s + d_t)^3)$ . In the

---

**Algorithm 1** Supervised and semi-supervised heterogeneous domain adaptation using CDSPP

---

**Input:** Labeled source data set  $\mathcal{D}^s = \{(\mathbf{x}_i^s, y_i^s)\}, i = 1, 2, \dots, n_s$  and labeled target data set  $\mathcal{D}^t = \{(\mathbf{x}_i^t)\}, i = 1, 2, \dots, n_t$ , the dimensionality of subspace  $d$ , number of iteration  $T$  if semi-supervised learning.

**Output:** The projection matrix  $\mathbf{P}_s$  and  $\mathbf{P}_t$  for source and target domains, the labels predicted for unlabeled target data  $\mathbf{X}^u$ .

**Training:**

- 1: Initialize  $k=1$ ;
- 2: Learn the projection  $\mathbf{P}_s^{(0)}$  and  $\mathbf{P}_t^{(0)}$  using labeled data  $\mathcal{D}^s \cup \mathcal{D}^t$  by solving the generalized eigenvalue problem in Eq.(7);
- 3: **if** semi-supervised **then**
- 4: Get the unlabeled target data set  $\mathcal{D}^u$ ;
- 5: **while**  $k \leq T$  **do**
- 6: Label all the samples from  $\mathcal{D}^u$  by Eq.(14);
- 7: Select a subset of (top  $kn_u/T$  most confident) pseudo-labeled target samples  $\mathcal{S}^{(k)} \subseteq \mathcal{D}^u$ ;
- 8: Learn  $\mathbf{P}_s^{(k)}$  and  $\mathbf{P}_t^{(k)}$  using a combination of labeled and pseudo-labeled data sets  $\mathcal{D}^s \cup \mathcal{D}^t \cup \mathcal{S}^{(k)}$ ;
- 9:  $k \leftarrow k + 1$ ;
- 10: **end while**
- 11: **end if**
- 12: Classify unlabeled target samples  $\mathbf{X}^u$  using Eq.(14).

---

case of semi-supervised HDA, the time complexity will be increased by  $T$  times and the value of  $n_t$  increases by the number of selected pseudo-labeled target samples in each iteration.

## 4. Experiments

To evaluate the effectiveness of the proposed method in heterogeneous domain adaptation, we conduct thorough experiments on commonly used benchmark datasets. We compare the proposed approach with existing HDA methods and analyze its sensitivity to hyper-parameters.

### 4.1. Datasets and Experimental Settings

**Office-Caltech** [10] is an image dataset containing four domains: Amazon (A), Webcam (W), DSLR (D) and Caltech (C) from 10 common classes. Two image features (i.e. 4096-dim Decaf<sub>6</sub> and 800-dim SURF) are used for cross-domain adaptation. **Multilingual Reuters Collection (MRC)** [1] is a cross-lingual text classification dataset containing 6 classes in 5 languages (i.e. EN, FR, GE, IT, SP). We follow the settings in [14] extracting BoW features and applying PCA to get heterogeneous feature dimensions (i.e. 1131, 1230, 1417, 1041, 807 respectively) for five domains. In our experiments, SP serves as the target domain and other four languages as the source domains respectively. As a result, we have four HDA tasks. **NUS-WIDE** [6] and **ImageNet** [7] datasets are employed for text to image domain adaptation. Following [5] we consider

Table 1: The statistics of datasets (notations: LSS/c – Labeled Source Samples per class; LTS/c – Labeled Target Sample per class; UTS/c – Unlabeled Target Samples per class; all – all samples except the ones chosen as labeled target samples).

Dataset	# Domain	# Task	# Class	# LSS/c	# LTS/c	# UTS/c
Office-Caltech	4	16	10	20	3	all
MRC	5	4	6	100	10	500
NUS-ImageNet	2	1	8	100	3	100
Office-Home	4	16	65	20	3	all

Table 2: Mean(std) of classification accuracy (%) over ten trials for cross-language and tag-to-image adaptation under supervised (denoted by \*) and semi-supervised settings (each column represents one Source → Target adaptation task).

Method	EN→SP	FR→SP	GE→SP	IT→SP	Avg	Tag→Image
SVM <sub>t</sub> *	67.0(2.4)	67.0(2.4)	67.0(2.4)	67.0(2.4)	67.0	60.6(6.0)
HFA [19] *	68.1(3.0)	68.0(3.0)	68.0(3.0)	68.0(3.0)	68.0	67.5(2.5)
CDLS_sup [14] *	63.0(3.6)	63.4(2.4)	64.0(2.2)	64.6(3.6)	63.8	66.3(3.9)
CDSPP_sup (Ours) *	67.2(2.8)	67.3(2.9)	67.3(2.9)	67.3(2.8)	67.3	67.2(3.0)
DAMA [26]	67.3(2.8)	66.9(2.9)	66.6(3.3)	66.7(2.9)	66.9	67.1(2.6)
SHFA [19]	66.9(3.7)	66.1(2.7)	67.5(3.1)	67.4(2.2)	67.0	68.1(2.7)
CDLS [14]	69.4(3.0)	69.4(3.0)	69.4(3.2)	69.3(3.1)	69.4	69.6(2.1)
Li et al. [16]	<b>71.4(2.9)</b>	<b>71.6(2.9)</b>	<b>71.7(3.0)</b>	<b>72.3(2.5)</b>	<b>71.7</b>	70.5(4.0)
TIT [17]	67.1(2.8)	67.6(2.6)	66.1(3.5)	67.8(2.0)	67.2	70.7(3.4)
STN [33]	67.1(3.6)	67.3(2.5)	66.9(3.5)	66.7(3.8)	67.0	74.3(5.2)
DAMA +	69.1(2.2)	68.6(3.7)	68.5(2.6)	68.7(2.6)	68.7	73.1(4.3)
CDSPP (Ours)	69.1(3.2)	69.0(3.6)	68.8(3.2)	68.8(3.0)	68.9	<b>74.7(3.4)</b>

8 overlapping classes using tag information represented by 64-dim features from NUS-WIDE as the source domain and 4096-dim Decaf<sub>6</sub> features of images from ImageNet as the target domain. However, the above datasets contain very limited numbers of classes and may not discriminate capabilities of different methods. We introduce **Office-Home** [25] containing four domains (i.e. Art, Clipart, Product and Real-world) as a new testbed for HDA. We use VGG16 [24] and ResNet50 [11] models pre-trained on ImageNet to extract 4096-dim and 2048-dim features. More details of the datasets and protocols used in our experiments are summarized in Table 1.

### 4.2. Comparative Study

To evaluate the effectiveness of the proposed CDSPP in different HDA problems, we conduct this comparative study and compare the performance of different state-of-the-art methods in different experimental settings. Specifically, we compare with SVM<sub>t</sub> (trained on the target dataset  $\mathcal{D}^t$  only), HFA [19] and CDLS\_sup [14] under the supervised HDA setting (i.e. the unlabeled target samples are not available during training). For semi-supervised HDA, we compare with DAMA [26], SHFA [19], CDLS [14], [16], TIT [17], STN [33] and DAMA+, our extension of DAMA by incorporating it into our iterative learning framework (c.f. Section 3.3). In all experiments, we use the optimal parameters suggested in the original papers for the comparative methods whilst set the hyper-parameters of CDSPP empirically as  $d$  equal to the number of classes in the dataset,  $\alpha = 10$  and  $T = 5$ . More details of hyper-parameter value selection will be discussed later.

Although there exist fixed experimental protocols in terms of the number of labeled samples used for training as shown in Table 1, there is no standard data splits publicly available to follow. As it will be demonstrated in our experimental results, selecting different samples for training can lead to significant performance variance. We generate data splits randomly in our

Table 3: Mean(std) of classification accuracy (%) over ten trials on the Office-Caltech dataset using SURF (source) and Decaf<sub>6</sub> (target) features under supervised (denoted by \*) and semi-supervised settings (each column represents one Source → Target adaptation task).

Method	C→C	C→A	C→D	C→W	A→C	A→A	A→D	A→W	D→C	D→A	D→D	D→W	W→C	W→A	W→D	W→W	Avg
SVM <sub>t</sub> *	73.6(4.9)	87.9(2.2)	92.3(3.6)	88.4(3.8)	73.6(4.9)	87.9(2.2)	92.3(3.6)	88.4(3.8)	73.6(4.9)	87.9(2.2)	92.3(3.6)	88.4(3.8)	73.6(4.9)	87.9(2.2)	92.3(3.6)	88.4(3.8)	85.5
HFA [19] *	80.1(2.3)	88.9(1.9)	91.6(3.6)	90.7(3.5)	80.2(2.3)	88.9(1.9)	91.5(3.6)	90.5(3.6)	80.2(2.2)	88.8(1.9)	91.8(3.6)	90.7(3.5)	80.2(2.3)	88.8(1.9)	91.5(3.7)	90.6(3.7)	87.8
CDLS <sub>sup</sub> [14] *	76.1(2.1)	86.6(3.2)	91.3(4.7)	87.4(3.5)	75.9(3.5)	87.0(2.8)	90.6(3.8)	86.0(3.6)	51.5(4.4)	74.2(2.4)	86.6(3.2)	77.2(5.1)	74.7(4.1)	85.4(3.0)	90.5(3.8)	86.0(3.5)	81.7
CDSPP <sub>sup</sub> (Ours) *	80.3(2.0)	89.0(1.9)	92.0(3.5)	90.7(3.8)	80.3(2.1)	89.1(1.9)	91.7(3.7)	90.7(3.7)	79.8(2.1)	88.9(1.8)	90.4(3.9)	90.1(3.9)	80.4(2.2)	89.0(1.8)	91.5(4.1)	90.6(3.8)	87.8
DAMA [26]	79.4(2.3)	88.3(1.9)	92.5(2.1)	90.0(4.3)	77.6(3.8)	86.5(1.8)	92.4(3.1)	89.8(4.2)	77.3(2.8)	89.6(1.3)	91.0(3.9)	90.7(4.2)	79.1(2.9)	88.6(1.5)	91.3(3.3)	89.9(4.5)	87.1
SHFA [19]	77.1(2.8)	86.2(3.8)	93.0(3.6)	90.0(2.6)	80.5(3.1)	86.7(2.2)	94.3(2.5)	90.0(4.0)	81.6(2.1)	88.5(2.9)	93.5(3.9)	92.0(4.1)	80.5(1.8)	88.5(2.4)	93.5(3.5)	89.5(4.2)	87.8
CDLS [14]	80.6(1.8)	88.8(2.1)	93.0(3.2)	91.1(3.7)	80.6(1.8)	88.8(2.1)	92.0(3.0)	91.0(4.5)	78.4(2.7)	87.2(2.3)	93.0(3.7)	88.9(5.6)	81.0(2.0)	88.6(2.2)	92.1(3.3)	91.4(4.2)	87.9
Li et al. [16]	87.2(1.1)	90.8(1.3)	92.9(3.3)	93.9(3.9)	87.0(1.1)	90.5(1.7)	94.7(2.5)	94.0(3.9)	87.0(1.3)	90.5(2.0)	94.5(2.8)	94.3(3.7)	87.0(1.3)	90.7(1.5)	93.4(4.1)	92.8(4.6)	91.3
TIT [17]	84.9(1.7)	89.9(1.6)	94.6(3.1)	92.2(4.3)	84.6(1.5)	89.7(1.7)	94.6(2.2)	92.3(4.9)	82.7(1.5)	88.7(1.9)	94.3(2.7)	92.1(4.0)	84.7(1.6)	89.5(1.8)	92.5(2.8)	92.5(4.3)	90.0
STN [33]	88.2(1.7)	92.4(0.7)	94.4(2.0)	92.8(4.9)	<b>88.4(1.6)</b>	92.5(0.7)	95.0(2.0)	93.9(4.1)	87.9(1.7)	92.2(0.5)	94.4(2.5)	93.3(5.0)	<b>88.2(1.8)</b>	92.6(0.8)	93.9(3.2)	92.2(5.1)	92.0
DAMA+	88.2(1.8)	<b>92.7(0.5)</b>	93.1(1.8)	90.2(4.7)	88.0(1.6)	<b>93.0(0.6)</b>	90.3(3.9)	92.3(4.6)	87.9(2.0)	<b>93.0(0.6)</b>	91.8(5.5)	92.5(3.6)	88.1(2.1)	<b>92.7(0.6)</b>	92.9(3.5)	93.8(3.5)	91.3
CDSPP (Ours)	<b>88.3(0.7)</b>	92.3(0.7)	<b>95.6(1.5)</b>	<b>94.1(4.1)</b>	88.1(1.0)	92.6(0.5)	<b>95.7(1.0)</b>	<b>94.6(3.8)</b>	<b>88.1(0.6)</b>	92.7(0.5)	93.5(4.6)	<b>94.7(3.5)</b>	88.1(1.0)	92.5(0.5)	<b>95.7(1.3)</b>	<b>94.3(3.8)</b>	<b>92.6</b>

Table 4: Mean(std) of classification accuracy (%) over ten trials on the Office-Home dataset using VGG16 (source) and ResNet50 (target) features under supervised (denoted by \*) and semi-supervised settings (each column represents one Source → Target adaptation task).

Method	A→A	A→C	A→P	A→R	C→A	C→C	C→P	C→R	P→A	P→C	P→P	P→R	R→A	R→C	R→P	R→R	Avg
SVM <sub>t</sub> *	51.8(1.2)	41.4(1.6)	71.0(1.4)	65.8(2.3)	51.8(1.2)	41.4(1.6)	71.0(1.4)	65.8(2.3)	51.8(1.2)	41.4(1.6)	71.0(1.4)	65.8(2.3)	51.8(1.2)	41.4(1.6)	71.0(1.4)	65.8(2.3)	57.5
CDLS <sub>sup</sub> [14] *	58.7(0.9)	45.7(1.5)	75.0(0.8)	69.8(1.9)	53.4(1.0)	48.6(1.0)	73.9(0.9)	67.8(1.8)	55.0(0.9)	45.9(1.4)	78.0(0.8)	70.2(1.5)	56.5(1.1)	46.8(1.5)	76.2(0.5)	72.4(1.4)	62.1
CDSPP <sub>sup</sub> (Ours) *	60.8(1.2)	49.5(1.1)	76.3(0.8)	71.9(1.8)	59.4(1.4)	50.4(1.0)	76.1(0.9)	71.6(1.8)	59.8(1.2)	49.6(1.1)	78.0(0.9)	72.4(1.4)	60.4(1.3)	49.8(0.9)	76.9(1.0)	73.3(1.6)	64.8
DAMA [26]	55.3(2.9)	43.3(1.1)	71.8(1.4)	66.8(3.5)	48.0(7.3)	39.4(6.1)	65.6(5.9)	61.4(3.4)	51.8(5.3)	41.0(3.5)	72.3(4.0)	61.8(4.9)	49.5(5.8)	37.5(5.1)	61.6(7.3)	61.8(6.5)	55.5
CDLS [14]	62.1(0.9)	46.9(1.2)	76.8(0.7)	71.5(2.3)	55.7(1.3)	47.4(1.2)	76.7(0.6)	70.8(2.0)	56.4(1.1)	47.0(1.2)	77.8(0.6)	71.5(2.0)	56.7(1.2)	47.6(1.3)	77.5(0.4)	72.2(2.0)	63.4
Li et al. [16]	59.8(1.2)	48.2(1.5)	80.0(1.2)	75.5(1.8)	59.8(1.1)	48.2(1.3)	80.0(1.3)	75.4(1.9)	59.5(1.5)	48.2(1.4)	80.0(1.6)	75.7(1.9)	59.6(1.3)	48.2(1.5)	79.9(1.4)	75.7(1.8)	65.8
TIT [17]	55.6(1.0)	44.7(1.3)	74.3(1.0)	70.3(1.8)	56.1(0.9)	45.5(1.1)	74.7(0.7)	70.2(1.7)	55.9(1.1)	45.3(1.3)	74.9(0.9)	70.2(1.8)	55.5(1.5)	44.6(1.4)	74.7(0.8)	69.9(2.0)	61.4
STN [33]	62.6(1.4)	51.2(1.5)	78.7(3.9)	74.5(4.3)	56.1(3.8)	52.2(2.2)	77.0(4.0)	71.1(6.0)	60.7(1.3)	49.3(6.0)	<b>82.4(1.0)</b>	75.8(2.8)	61.0(1.3)	50.6(3.2)	80.4(0.9)	75.7(4.4)	66.2
DAMA+	60.7(2.7)	48.9(1.8)	78.1(1.5)	75.1(2.2)	58.3(4.7)	46.4(4.8)	75.9(4.4)	72.3(2.0)	59.8(3.6)	46.3(3.9)	78.4(2.3)	71.8(3.8)	58.2(3.8)	44.1(4.5)	72.6(3.8)	70.6(4.5)	63.6
CDSPP (Ours)	<b>65.7(1.0)</b>	<b>54.8(2.0)</b>	<b>81.0(1.5)</b>	<b>78.4(1.1)</b>	<b>65.0(1.4)</b>	<b>55.1(1.6)</b>	<b>80.9(1.6)</b>	<b>78.5(1.2)</b>	<b>65.6(0.4)</b>	<b>54.7(1.9)</b>	81.5(1.1)	<b>78.8(1.0)</b>	<b>65.5(0.9)</b>	<b>54.6(1.6)</b>	<b>80.9(1.6)</b>	<b>79.4(0.9)</b>	<b>70.0</b>

Table 5: Mean(std) of classification accuracy (%) over ten trials on the Office-Home dataset using ResNet50 (source) and VGG16 (target) features under supervised (denoted by \*) and semi-supervised settings (each column represents one Source → Target adaptation task).

Method	A→A	A→C	A→P	A→R	C→A	C→C	C→P	C→R	P→A	P→C	P→P	P→R	R→A	R→C	R→P	R→R	Avg
SVM <sub>t</sub> *	40.3(1.4)	30.5(1.6)	63.3(1.7)	56.3(2.9)	40.3(1.4)	30.5(1.6)	63.3(1.7)	56.3(2.9)	40.3(1.4)	30.5(1.6)	63.3(1.7)	56.3(2.9)	40.3(1.4)	30.5(1.6)	63.3(1.7)	56.3(2.9)	47.6
CDLS <sub>sup</sub> [14] *	51.4(1.1)	36.5(1.0)	69.6(1.1)	63.5(2.0)	46.4(1.2)	39.2(1.0)	68.7(1.2)	62.0(1.6)	47.2(1.2)	36.4(0.8)	73.1(1.0)	64.6(1.9)	48.6(1.1)	37.1(1.1)	70.9(1.2)	66.4(2.0)	55.1
CDSPP (Ours) *	49.7(1.1)	39.2(1.0)	69.5(1.3)	63.7(2.0)	48.3(1.2)	40.4(1.3)	69.5(1.5)	63.4(1.8)	48.5(1.1)	38.9(0.8)	71.3(1.4)	64.1(1.9)	49.0(1.2)	39.4(1.1)	70.1(1.3)	65.0(2.1)	55.6
DAMA [26]	45.6(2.7)	34.5(2.0)	64.8(3.2)	58.7(3.1)	43.4(2.3)	32.9(3.5)	63.1(2.0)	57.9(3.3)	43.4(4.4)	32.6(4.4)	61.3(5.0)	58.2(3.2)	43.3(5.0)	30.8(3.5)	58.9(4.2)	55.8(4.5)	49.1
CDLS [14]	54.9(1.1)	36.6(1.1)	71.1(0.8)	65.9(1.3)	47.8(1.4)	39.8(1.2)	69.5(1.2)	63.6(1.4)	49.7(1.2)	36.8(1.2)	75.6(0.8)	67.9(1.6)	52.3(1.0)	38.5(1.3)	73.1(1.0)	69.6(1.6)	57.0
Li et al. [16]	51.4(1.0)	38.3(1.3)	73.7(1.2)	67.4(1.6)	51.2(1.4)	38.2(1.2)	73.6(1.2)	67.4(1.6)	51.2(1.1)	38.1(1.4)	73.6(1.2)	67.3(1.9)	51.2(0.9)	38.2(1.2)	73.7(1.2)	67.4(1.4)	57.6
TIT [17]	46.8(1.7)	36.4(1.2)	69.4(0.9)	62.5(1.8)	47.0(1.7)	36.4(1.1)	69.3(1.1)	62.0(2.2)	46.8(1.7)	36.4(1.1)	69.8(0.9)	62.4(2.1)	45.9(1.6)	36.0(1.3)	69.4(1.2)	62.5(2.1)	53.7
STN [33]	52.6(1.5)	41.2(2.4)	74.9(1.0)	69.2(1.5)	51.2(1.1)	42.5(1.2)	75.3(1.2)	69.6(1.0)	53.0(1.2)	41.7(1.4)	<b>77.3(1.2)</b>	70.7(1.4)	52.7(1.9)	41.7(1.4)	<b>76.6(1.0)</b>	71.6(1.3)	60.1
DAMA+	48.2(3.5)	36.6(2.5)	70.6(1.4)	63.8(2.7)	48.6(2.5)	33.9(3.9)	69.4(1.4)	64.3(3.1)	47.0(0.4)	33.3(5.8)	66.9(3.2)	62.8(3.8)	47.6(4.6)	31.7(4.3)	65.8(3.5)	59.9(4.3)	53.2
CDSPP (Ours)	<b>55.6(1.1)</b>	<b>44.7(1.8)</b>	<b>75.2(1.6)</b>	<b>71.7(1.4)</b>	<b>54.5(1.2)</b>	<b>46.0(1.6)</b>	<b>75.7(1.6)</b>	<b>71.4(1.9)</b>	<b>54.7(1.2)</b>	<b>45.0(1.6)</b>	76.0(1.8)	<b>71.8(1.6)</b>	<b>55.0(1.3)</b>	<b>44.9(2.0)</b>	75.8(1.8)	<b>72.1(1.8)</b>	<b>61.9</b>

experiments<sup>1</sup>. To mitigate the biases caused by the data selection, ten random data splits are generated for each adaptation task. We report the mean and standard deviation of the classification accuracy over these ten trials for each adaptation task. The results for all comparative methods are reproduced using the same data splits for a direct comparison. The implementations released by the authors are employed in our experiments. As a result, the results in this paper are not comparable with those reported in other papers since different sample selections have been used in our experiments. Our experimental results of both supervised and semi-supervised HDA on four datasets are shown in Tables 2-5 from which we can draw the following insights.

Table 2 (except the last column) lists the comparison results on the MRC dataset. The baseline method  $\text{SVM}_t$  achieves an accuracy of 67.0%<sup>2</sup> using only 10 labeled target domain samples per class for training. The labeled source domain data can benefit the performance with proper domain adaptation but the improvement is marginal for both HFA and our proposed CDSPP. The supervised version of CDLS uses PCA to learn a subspace from the target domain, hence the dimensionality of subspace cannot be higher than  $n_t - 1$ . Due to such limitation, CDLS<sub>sup</sub> performs worse than others when the number of labeled target samples is small which is usually the case for HDA problems. For the semi-supervised HDA, DAMA and SHFA perform no better than the baseline method  $\text{SVM}_t$  which was also observed in existing works [14, 16, 17]. The best performance (71.7%) is achieved by Li et al. [16] and our proposed CDSPP is the marginally worse with the average classification accuracy of 68.9%.

Table 2 (rightmost column) also presents the results of tag-to-image adaptation on the NUS-ImageNet dataset. There is only one adaptation task (i.e. Tag  $\rightarrow$  Image) in this dataset. In the supervised HDA setting, the baseline method  $\text{SVM}_t$  is outperformed by all three comparative methods with large margins among which HFA achieves the best performance of 67.5% as opposed to the accuracy of 67.2% by CDSPP. However, HFA is more computationally expensive than others as discussed in [19]. In the semi-supervised HDA setting, our method achieves the best performance with the accuracy of 74.7%.

Similar results can also be observed in Table 3 for the image classification experiments on Office-Caltech. Both HFA and our CDSPP achieve the same average accuracy of 87.8% in the supervised HDA setting. CDLS<sub>sup</sub> performs worse than the baseline method  $\text{SVM}_t$  again due to the restricted PCA dimensions as discussed above. In the semi-supervised HDA, our CDSPP achieves the best results in 9 out of 16 adaptation tasks and has the highest average accuracy of 92.6%.

The experimental results for the challenging Office-Home dataset are shown in Table 4 and Table 5. The difference between these two tables lies in the features used for the source/target domains are VGG16/ResNet50 and

ResNet50/VGG16 respectively. In this experiment, the methods HFA and SHFA are excluded due to their extremely long computation time given the scale of this dataset. It can be seen that CDLS<sub>sup</sub>, for the first time, outperforms the baseline method  $\text{SVM}_t$  on this dataset since the total number of labeled target samples is 195 which no longer restricts the PCA dimension in this algorithm. In both tables, the best performances were achieved by our CDSPP for most adaptation tasks in both supervised and semi-supervised settings. Specifically, CDSPP achieves an average accuracy of 70.0% when VGG16 and ResNet50 features were employed for source and target domains, significantly better than the second best performance 66.2% achieved by STN Yao et al. [33]. Similar results can be observed in Table 5, CDSPP achieves the best performance of 61.9% as opposed to the second best 60.1% by STN Yao et al. [33].

In addition, the performance comparison between DAMA and DAMA+ provide evidence that the use of iterative learning framework described in Section 3.3 is beneficial to semi-supervised HDA. On the other hand, the superior performance of CDSPP to DAMA+ across all datasets validates the fact that our CDSPP is essentially different from DAMA as discussed in Section 3.2.

#### 4.3. On the Number of Labeled Target Samples

We conducted additional experiments of semi-supervised HDA to compare our proposed CDSLPP with other methods when different numbers of labeled target samples were used for training. Specifically, we set the number of labeled target samples as 5, 10, 15 or 20 for the MRC dataset whilst for the other three datasets the investigated numbers of labeled target samples were within the collection of {1, 3, 5, 7, 9}. For the MRC and NUS-ImageNet datasets, all adaptation tasks (i.e.  $EN/FR/GE/IT \rightarrow SP$  and  $Tag \rightarrow Image$ , respectively) were repeated for ten trials with randomly selected data (the same as those used in the previous experiment). To save computational time without loss of generality, we only conducted the first four adaptation tasks for the first three trials for the Office-Caltech ( $C \rightarrow C, C \rightarrow A, C \rightarrow D, C \rightarrow W$ ) and Office-Home ( $A \rightarrow A, A \rightarrow C, A \rightarrow P, A \rightarrow R$  with VGG16 and ResNet50 as the source and target features, respectively) datasets in this experiment. For each dataset, the average classification accuracy over all the conducted adaptation tasks in this dataset is reported for comparison.

The experimental results are shown in Figure 2 from which we can draw some conclusions. (1) The performance of all methods is improved with the increase of labeled target samples since more labeled target samples provide additional information for the training. (2) The performance margins between different methods decrease when more labeled target samples are used for training. This phenomenon demonstrates these methods have different capabilities of cross-domain knowledge transfer which is of vital importance when there are limited labeled data in the target domain. (3) Our proposed CDSPP algorithm outperforms the others in three out of four datasets regardless of the number of labeled target samples. The superiority of CDSPP to other methods is more significant when less

<sup>1</sup>The data splits and code are released: <https://github.com/hellowangqian/cdspp-hda>.

<sup>2</sup> $\text{SVM}_t$  uses only labeled target samples for training and the results should be the same regardless of the source domains.

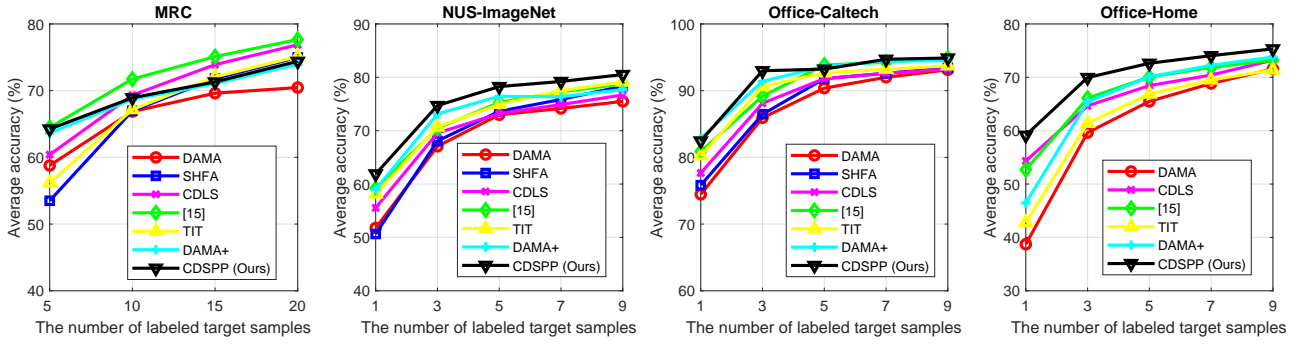


Figure 2: Comparison results when different numbers of labeled target samples are used.

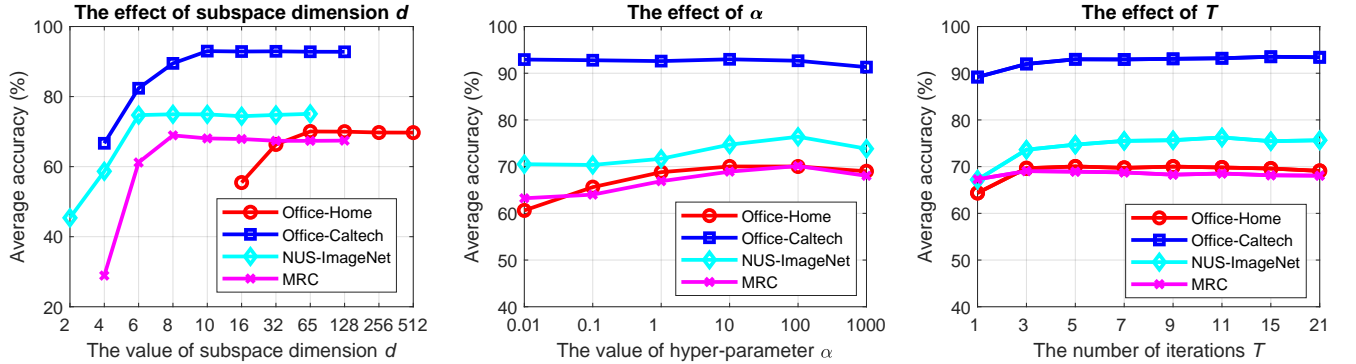


Figure 3: Performance sensitivity to hyper-parameters.

labeled target samples are available. (4) On the MRC dataset, our method performs the best when 5 labeled target samples are used but outperformed by CDLS [14] and [16] when more labeled target samples are available.

#### 4.4. On the Effect of Hyper-parameters

In all our experiments described above, we empirically set the dimensionality of the common subspace  $d$  equal to the number of classes in the dataset and set the hyper-parameters  $\alpha = 10$  (c.f. Eq.(7)) and the number of iterations  $T = 5$  (c.f. Algorithm 1). In this experiment, we will show how these values were selected and the fact that our algorithm is not sensitive to these hyper-parameters across all the datasets. Similar to the experimental settings in the previous section, we repeated all the adaptation tasks for ten trials for the MRC and NUS-ImageNet datasets and repeated the first four adaptation tasks for the first three trials for the Office-Caltech and Office-Home datasets to save time without loss of generality. The average accuracy over all the investigated adaptation tasks is reported for each dataset when a specific hyper-parameter value is used.

Firstly, we investigate the effect of the subspace dimension  $d$ . The values of  $d$  were from the set  $\{2, 4, 6, 8, 10, 16, 32, 64/65, 128, 256, 512\}$  which contains the class numbers of four datasets (i.e. 6, 8, 10 and 65) as well as other candidate values less or greater than the class numbers. The experimental results are shown in the left graph of Figure 3.

It is not hard to see that the best performance can be achieved when the value of  $d$  is no less than the number of classes in each dataset. A greater value of  $d$  does not further improve the performance but a smaller value of  $d$  leads to a significant performance drop. As a result, it is easy to select an optimal value of the subspace dimension for our proposed CDSPP.

Subsequently, We investigate the effect of the regularization parameter  $\alpha$  in Eq.(7) by conducting experiments with the values of  $\alpha$  selected from  $\{0.01, 0.1, 1, 10, 100, 1000\}$ . The experimental results are shown in the middle graph of Figure 3 from which we can see that the optimal values of  $\alpha$  should be between 10 and 100 across all datasets. A smaller value of  $\alpha$  leads to performance drops for all datasets except Office-Caltech. This validates the necessity of the regularization term in Eq.(7) in our method and it is not very sensitive to the value of  $\alpha$ . Similar findings have been validated in traditional LPP algorithm by Wang and Chen [30].

Finally, we were concerned about the number of iterations  $T$  by setting  $T = \{1, 3, 5, 7, 9, 11, 15, 21\}$ . The right-side graph in Figure 3 shows that the CDSPP algorithm performs generally well when  $T \geq 5$ . Increasing the number of iterations further can only improve the performance on the NUS-ImageNet dataset very marginally but will increase the computational cost significantly. As a result, we selected  $T = 5$  as the optimal value in all our experiments.

## 5. Conclusion

We propose a novel algorithm CDSPP for HDA and extend it to the semi-supervised setting by incorporating it into an iterative learning framework. Experimental results on several benchmark datasets demonstrate the proposed CDSPP is not only computationally efficient but also can achieve state-of-the-art performance on four datasets. We also investigate the effect of the number of labeled target samples in the performance of different methods and found that the use of too many labeled target samples will suppress the performance distinction among different methods. The newly introduced benchmark dataset Office-Home for HDA is proved a proper testbed for HDA since it is more challenging with much more classes than others and the performances of investigated methods on this dataset are more significantly varied. In addition, the proposed method for HDA is not sensitive to hyper-parameters and it is easy to select optimal hyper-parameter values across varying datasets.

## References

- [1] Amini, M., Usunier, N., and Goutte, C. (2009). Learning from multiple partially observed views—an application to multilingual text categorization. In *NeurIPS*, pages 28–36.
- [2] Atapour-Abarghouei, A. and Breckon, T. P. (2018). Real-time monocular depth estimation using synthetic data with domain adaptation via image style transfer. In *CVPR*, pages 2800–2810.
- [3] Chen, C., Chen, Z., Jiang, B., and Jin, X. (2019a). Joint domain alignment and discriminative feature learning for unsupervised deep domain adaptation. In *AAAI*.
- [4] Chen, C., Xie, W., Huang, W., Rong, Y., Ding, X., Huang, Y., Xu, T., and Huang, J. (2019b). Progressive feature alignment for unsupervised domain adaptation. In *CVPR*, pages 627–636.
- [5] Chen, W.-Y., Hsu, T.-M. H., Tsai, Y.-H. H., Wang, Y.-C. F., and Chen, M.-S. (2016). Transfer neural trees for heterogeneous domain adaptation. In *ECCV*, pages 399–414. Springer.
- [6] Chua, T.-S., Tang, J., Hong, R., Li, H., Luo, Z., and Zheng, Y. (2009). Nus-wide: a real-world web image database from national university of singapore. In *ACM international conference on image and video retrieval*, page 48.
- [7] Deng, J., Dong, W., Socher, R., Li, L.-J., Li, K., and Fei-Fei, L. (2009). Imagenet: A large-scale hierarchical image database. In *CVPR*, pages 248–255.
- [8] Deng, W.-Y., Dong, Y.-Y., Liu, G.-D., Wang, Y., and Men, J. (2019). Multiclass heterogeneous domain adaptation via bidirectional ecoc projection. *Neural Networks*, 119:313–322.
- [9] Fang, W.-C. and Chiang, Y.-T. (2018). A discriminative feature mapping approach to heterogeneous domain adaptation. *Pattern Recognition Letters*, 106:13–19.
- [10] Gong, B., Shi, Y., Sha, F., and Grauman, K. (2012). Geodesic flow kernel for unsupervised domain adaptation. In *CVPR*, pages 2066–2073. IEEE.
- [11] He, K., Zhang, X., Ren, S., and Sun, J. (2016). Deep residual learning for image recognition. In *CVPR*, pages 770–778.
- [12] He, X. and Niyogi, P. (2004). Locality preserving projections. In *NeurIPS*, pages 153–160.
- [13] Huang, J., Zhou, Z., Shang, J., and Niu, C. (2020). Heterogeneous domain adaptation with label and structural consistency. *Multimedia Tools and Applications*, pages 1–21.
- [14] Hubert Tsai, Y.-H., Yeh, Y.-R., and Frank Wang, Y.-C. (2016). Learning cross-domain landmarks for heterogeneous domain adaptation. In *CVPR*, pages 5081–5090.
- [15] Li, H., Pan, S. J., Wan, R., and Kot, A. C. (2019). Heterogeneous transfer learning via deep matrix completion with adversarial kernel embedding. In *AAAI*.
- [16] Li, J., Lu, K., Huang, Z., Zhu, L., and Shen, H. T. (2018a). Heterogeneous domain adaptation through progressive alignment. *IEEE transactions on neural networks and learning systems*, 30(5):1381–1391.
- [17] Li, J., Lu, K., Huang, Z., Zhu, L., and Shen, H. T. (2018b). Transfer independently together: a generalized framework for domain adaptation. *IEEE transactions on Cybernetics*, 49(6):2144–2155.
- [18] Li, J., Lu, K., Zhu, L., and Li, Z. (2017). Locality-constrained transfer coding for heterogeneous domain adaptation. In *Australasian database conference*, pages 193–204. Springer.
- [19] Li, W., Duan, L., Xu, D., and Tsang, I. W. (2013). Learning with augmented features for supervised and semi-supervised heterogeneous domain adaptation. *IEEE transactions on PAMI*, 36(6):1134–1148.
- [20] Mozafari, A. S. and Jamzad, M. (2016). A svm-based model-transferring method for heterogeneous domain adaptation. *Pattern Recognition*, 56:142–158.
- [21] Patel, V. M., Gopalan, R., Li, R., and Chellappa, R. (2015). Visual domain adaptation: A survey of recent advances. *IEEE signal processing magazine*, 32(3):53–69.
- [22] Petersen, K. B., Pedersen, M. S., et al. (2008). The matrix cookbook. *Technical University of Denmark*, 7(15):510.
- [23] Shen, C. and Guo, Y. (2018). Unsupervised heterogeneous domain adaptation with sparse feature transformation. In *ACML*, pages 375–390.
- [24] Simonyan, K. and Zisserman, A. (2015). Very deep convolutional networks for large-scale image recognition. In *ICLR*.
- [25] Venkateswara, H., Eusebio, J., Chakraborty, S., and Panchanathan, S. (2017). Deep hashing network for unsupervised domain adaptation. In *CVPR*, pages 5018–5027.
- [26] Wang, C. and Mahadevan, S. (2011). Heterogeneous domain adaptation using manifold alignment. In *IJCAI*.
- [27] Wang, J., Feng, W., Chen, Y., Yu, H., Huang, M., and Yu, P. S. (2018). Visual domain adaptation with manifold embedded distribution alignment. In *ACMMM*, pages 402–410.
- [28] Wang, Q. and Breckon, T. P. (2020). Unsupervised domain adaptation via structured prediction based selective pseudo-labeling. In *AAAI*.
- [29] Wang, Q., Bu, P., and Breckon, T. P. (2019). Unifying unsupervised domain adaptation and zero-shot visual recognition. In *IJCNN*.
- [30] Wang, Q. and Chen, K. (2017). Zero-shot visual recognition via bidirectional latent embedding. *International Journal of Computer Vision*, 124(3):356–383.
- [31] Weiss, K., Khoshgoftaar, T. M., and Wang, D. (2016). A survey of transfer learning. *Journal of Big Data*, 3(1):9.
- [32] Yan, Y., Li, W., Ng, M. K., Tan, M., Wu, H., Min, H., and Wu, Q. (2017). Learning discriminative correlation subspace for heterogeneous domain adaptation. In *IJCAI*, pages 3252–3258.
- [33] Yao, Y., Zhang, Y., Li, X., and Ye, Y. (2019). Heterogeneous domain adaptation via soft transfer network. In *ACMMM*, pages 1578–1586.
- [34] Zhang, Y., Tang, H., Jia, K., and Tan, M. (2019). Domain-symmetric networks for adversarial domain adaptation. In *CVPR*, pages 5031–5040.
- [35] Zhao, S., Li, B., Yue, X., Gu, Y., Xu, P., Hu, R., Chai, H., and Keutzer, K. (2019). Multi-source domain adaptation for semantic segmentation. In *NeurIPS*, pages 7285–7298.
- [36] Zhou, H. and Chen, K. (2019). Transferable positive/negative speech emotion recognition via class-wise adversarial domain adaptation. In *ICASSP*, pages 3732–3736.
- [37] Zhou, J. T., Pan, S. J., and Tsang, I. W. (2019a). A deep learning framework for hybrid heterogeneous transfer learning. *Artificial Intelligence*.
- [38] Zhou, J. T., Tsang, I. W., Pan, S. J., and Tan, M. (2019b). Multi-class heterogeneous domain adaptation. *Journal of Machine Learning Research*, 20(57):1–31.